ELSEVIER

Ceramics International 26 (2000) 237–243

CERAMICS INTERNATIONAL

Preparation and characterisation of lanthanum nickel strontium oxides by combined coprecipitation and molten salt reactions

Chen-Feng Kao*, Charng-Lih Jeng

Department of Chemical Engineering, National Cheng Kung University, Tainan, 70101, Taiwan

Received 22 March 1999; received in revised form 16 April 1999; accepted 1 June 1999

Abstract

Lanthanum nickel strontium oxides have been prepared by combined precipitation and molten salt reactions at 1073 K to obtain fine lanthanum nickel strontium oxides with a uniform particle size at 0.1 μm. The Sr^{2+}-doped $LaNiO_3$ is more stable at high temperature than the undoped one. The powders coprecipitated with sodium hydroxide have good sinterability leading to lower electrical resistivity for La_2NiO_4 than for $LaNiO_3$. Sr^{2+}-doping of La_2NiO_4 to $La_{2(1-x)}NiSr_{2x}O_4$ could reduce the electrical resistivity from 2.80×10^{-3} Ω•m ($x=0$) to 3.16×10^{-4}Ω•m ($x=0.30$). These compounds with different compositions exhibit the characteristics of Pauli paramagnetic materials. In correspondence with the change of phase ratios there are also changes in the mass susceptibility for $LaNiO_3$ from 2.23×10^{-6} (emu/Gauss-g) to 4.17×10^{-6} (emu/Gauss-g). © 2000 Elsevier Science Ltd and Techna S.r.l. All rights reserved.

Keywords: Synthesis; Characterisation; $La_{2(1-x)}NiSr_{2x}O_4$, $La_{1-x}NiSr_xO_3$

1. Introduction

$LaNiO_3$ is a cubic or rhombohedrally distorted perovskite-type structure. It has attracted much attention in the past few years, as a conducting layer for application in ferroelectric memories. $LaNiO_3$ is a semiconductor material in the electrode for high temperature fuel cells [1,2], as a catalyst [3–6] and as a sensor for ethanol. [7,8]. Its thermal stability is not so high (1170K) [9,10], and it is proven to be the perovskite structure [11–14]. It contains Pauli paramagnetic and metallic behaviour. Part of Ni^{3+} is reduced to Ni^{2+} due to the influence of oxygen partial pressure during heating. Therefore, $LaNiO_3$ is converted to La_2NiO_4, as a two-dimensional structure of K_2NiF_4 [15,16]. Kao et al. [17] have studied the preparation and characterisation of fine lanthanum nickel oxides by molten salt reactions. The substitution of La^{3+} in $LaNiO_3$ by Sr^{2+} would reduce the Ni^{3+} change to Ni^{2+} for assuring the cubic provskite structure [18]. For more precise recognition of doping behaviour, the Sr^{2+} was also doped into La_2NiO_4 for research completely [19,20].

In this research, we investigated the electrical and magnetic properties of the lanthanum nickel strontium oxides ($La_{2(1-x)}NiSr_{2x}O_4$, $La_{1-x}NiSr_xO_3$). There is not seen the study for the preparation of the lanthanum nickel strontium oxides by combined coprecipitation and molten salt reactions until now. Using this above method one can obtain the lanthanum nickel strontium oxide in lower temperature and produce uniform ceramic powders. Therefore, this method is more efficient and will be more popular to the application of materials.

We also study the system further, and analyze the effect of homogeneity, particle size distribution, calcining temperature and formation of phase from the precursors derived by chemical coprecipitation. Finally, from this investigation the concentration limits on the preparation in air and the electrical properties of the solid solution $La_{2(1-x)}NiSr_{2x}O_4$ ($0\leqq x\leqq1.0$) was determined.

Coprecipitation and molten salt reaction was used to form lanthanum nickel strontium oxides. The concept of this method is that salt, such as NaCl, that is formed as by product during co-precipitation was not washed out. The advantage of this method was discussed in detail [17]. Based on the previous process but alcohol was used as a coprecipited solvent for easy drying and recovery purposes. This process control is much easier than any other, and the dissolved salt is as an auxiliary

* Corresponding author.
E-mail address: cfkao@mail.ncku.edu.tw (C-F. Kao).

0272-8842/00/$20.00 © 2000 Elsevier Science Ltd and Techna S.r.l. All rights reserved.
PII: S0272-8842(99)00048-6

agent in reaction. The oxides from this method have more uniform and much better particle size distribution than that of solid-state reaction [21,22] or general chemical coprecipitation [23–28]. The general chemical coprecipitation process needs to wash the precursors with distilled water and to filtrate repeatedly that would make serious deviations from stoichiometry.

The reactions in this study can be written as follows:

$$2(1-x)LaCl_3 + NiCl_2 + 2xSrCl_2 + (8-2x)NaOH \rightarrow 2(1-x)La(OH)_3 + Ni(OH)_2 + 2xSr(OH)_2 + (8-2x)NaCl + x/2O_2 \rightarrow La_{2(1-x)}NiSr_{2x}O_4 + (8-2x)NaCl + (4-x)H_2O \uparrow$$

Owing to the existence and function of liquid melting salt, one can effectively give much more uniformity to enhance the reaction rate over those of the general chemical coprecipitation and solid-state reaction.

2. Experimental

A mixture with different ratio of lanthanum chloride (Fisher Scientific Company, certified), nickel chloride (Ferak GR.) and strontium chloride (Strem Chemicals) was dissolved in absolute ethyl alcohol and diluted to 0.2 M solution with absolute ethyl alcohol. Saturated sodium hydroxide aqueous solution was used to mix with the above solution to form a lanthanum nickel strontium hydroxide precursor. The rotary evaporator (Rotavapor R110, Buchi, Switzerland) was succeeded to obtain the dry precursors and to recovery the alcohol for reuse. Direct burning out alcohol for drying was also proceeded for comparing with rotary evaporation process.

Drying solid-phase precursors were calcined at 700, 800 and 900°C for 8 h, respectively. The salt was acted as a flux to improve the reactivity of precursor. The calcined powders were washed with distilled water and filtered repeatedly to obtain fine oxide particles. The silver nitrate solution was used to prove chloride ion existent in the oxide or not.

Fig. 1 shows the flow chart for the process in this study. 0.04 g dry precursors were proceeded to analyze by a Setaram TG/DTA 92 thermogravimetric apparatus. X-ray diffractometer (XRD) with Cu K_α radiation was used to identify the phases of oxides. The powders were dispersed in ethanol then few droplets were dipped out with a pipette into a filter paper. Cut off a small piece to be plated with gold for SEM examination. A JEOL JSM-35 scanning electron microscope (SEM) was employed to study the particle morphology. Superconducting quantum interference device (SQUID, Quantum Design MPMS7) magnetometer was performed

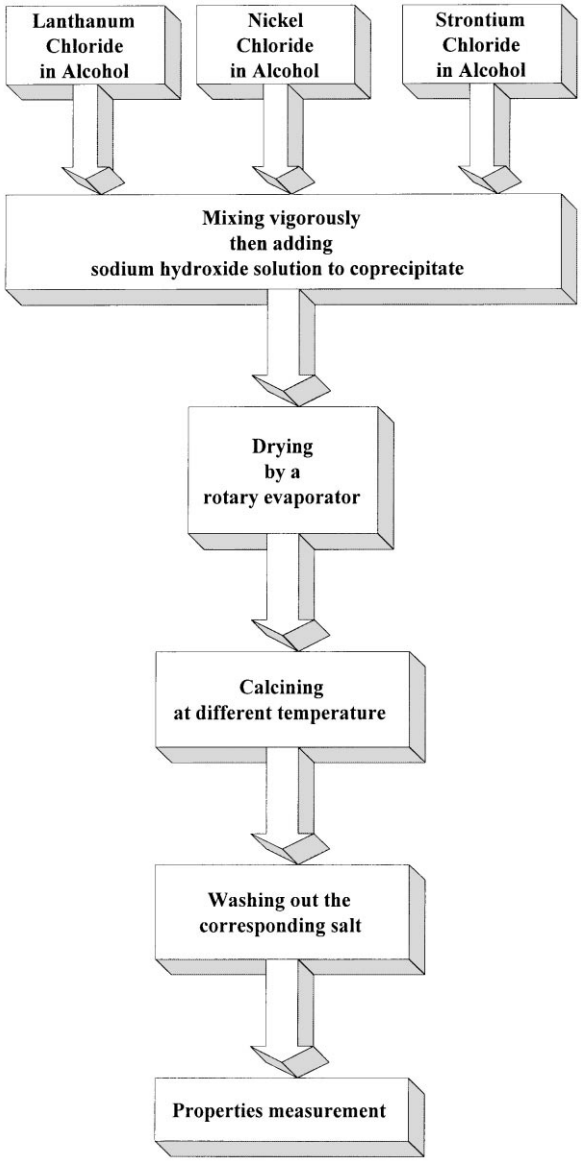

Fig. 1. Flow chart for preparation of lanthanum nickel strontium oxide.

magnetic measurement of the oxides in the temperature range 10–400 K [29]. The BET surface area of the oxide powders were measured with a BET analyzer (Micromeritics ASAP 2000, USA). The powders after pressing under 200 MPa were sintered at 1473 K. The conductivities of the bulk samples of the oxides were measured with a Digital Electrometer (Advantest Co. TR-8652 type).

3. Results and discussion

3.1. Thermogravity and calcining

The typical thermogravimetric analysis (TGA) and differential thermal analysis (DTA) curves, shown in

Fig. 2, are in agreement with the combined thermal behaviours of the hydroxide precursors. The endothermal peak at 583 K for nickel hydroxide and at 643 K for lanthanum hydroxide corresponds to their thermal decomposition. These results established that the coprecipitates consisted of both lanthanum and nickel hydroxides. That the endothermal peak at 1073 K is the melting point of sodium chloride [30–33]. So the calcining temperature was set at a heating rate of 10 K/min and maintained at 973, 1073 or 1173 K for 8 h, respectively. Then the precursors were calcined to become the desired oxides.

3.2. SEM analysis of the powders

The coprecipitated powders are mostly the agglomeration of small particles. This phenomenon is caused by loosing large amount of solvent from drying powders [34–36]. There is also agglomeration due to the existence of NaCl that could be examined easily from the precursors by XRD and polarized microscope analysis. Agglomeration is not a severe problem for the precursors to decompose into fine particle after calcining. The salts would be at the surface of oxides and be easy to be washed out.

The SEM analyses of the calcined powders were shown in Fig. 3, the uniformity of these calcined powders is better than that of the coprecipitated powders, and the degree of agglomeration of the calcined particle is less. The shape of the particle is mostly square and its particle size distribution is also more uniform, particles are crystalline and the particle size is at $(0.10 \pm 0.05)\mu m$.

3.3. BET analysis of the calcined powder

The BET surface area of $LaNiO_3$ and La_2NiO_4 were 5.3156 (m^2/g) and 24.5857 (m^2/g) made by BET method, respectively. This implies that $LaNiO_3$ particle is larger than La_2NiO_4 and it is in agreement with the SEM analysis (Fig. 3). The results of BET analysis showed a multilayer adsorption behaviour and could provide for the application of catalyst, such as methanation of carbon dioxide [3].

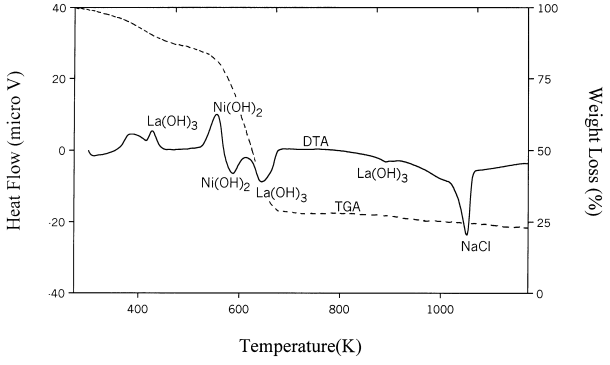

Fig. 2. Results of TGA and DTA analyses of lanthanum nickel strontium oxide.

3.4. XRD analysis of the calcined powder and sintered body

The results of some XRD analysis were shown in Fig. 4 ($La_{1-x}NiSr_xO_3$) and Fig. 5 ($La_{2(1-x)}NiSr_{2x}O_4$). From Fig. 4 the provskite phase $LaNiO_3$ were retained until the doping amount of Sr^{2+} beyond 0.15 then a trace of NiO appaered. The $La_{1.5}NiSr_{0.5}O_4$ and NiO contents were increased when the Sr^{2+} doping was at 0.5. Sr^{2+} doping from 0.75 to 1.00 there are NiO, SrO,Ni_2O_3 and $SrNiO_3$ to be become the mixing compounds. Fig. 5 showed that the mixing type compounds did not appear till Sr^{2+} doping was 0.15. In summary, the limit of doping amount was $x = 0.30$ for $La_{1-x}NiSr_xO_4$ and $x = 0.15$ for $La_{2(1-x)}NiSr_{2x}O_4$, respectively. For a further value of x the new compound appeared to be the mixing compounds of $La_{1.5}NiSr_{0.5}O_4$, SrO, $SrNiO_3$, NiO and Ni_2O_3.

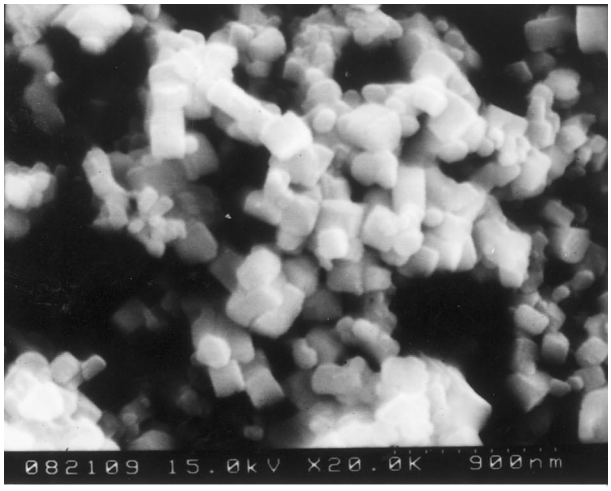

(a)

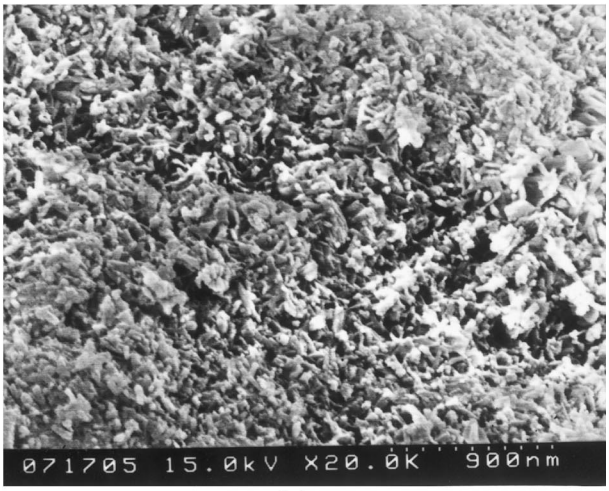

(b)

Fig. 3. SEM images for (a)$LaNiO_3$ and (b)La_2NiO_4 that were calcined at 1073 K for 8 h.

Fig. 6(a) represents the XRD pattern for $LaNiO_3$ and Fig 6(b) shows that $LaNiO_3$ had been sintered at 1473 K. The $LaNiO_3$ was converted to La_2NiO_4, due to the rising temperature for Ni^{3+} changing to Ni^{2+}. Fig. 6(c) showed the $LaNiO_3$ that doping Sr^{2+} would maintain its perovskite phase at 1473K. Owing to the effect of doping Sr^{2+} that could reduce the Ni^{3+} into Ni^{2+}. In this study the $LaNiO_3$ phase could be kept at 1473K when Sr^{2+} doping was at 0.04 but little amount of NiO and La_2NiO_4 were still predicable from Fig. 6(b) and (c).

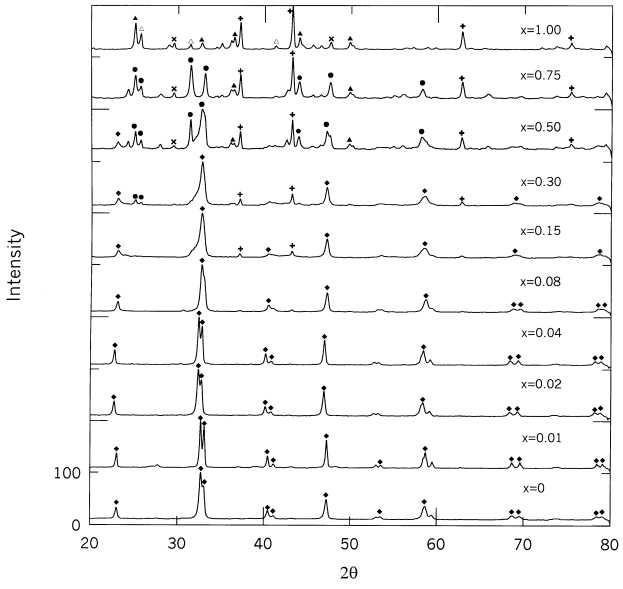

Fig. 4. XRD analyses for $La_{1-x}NiSr_xO_3$ with different x that calcined at 1073 K for 8 h. (◆ $LaNiO_3$, ● $La_{1.5}NiSr_{0.5}O_4$, + NiO, × SrO, ▲ $SrNiO_3$, △ Ni_2O_3.).

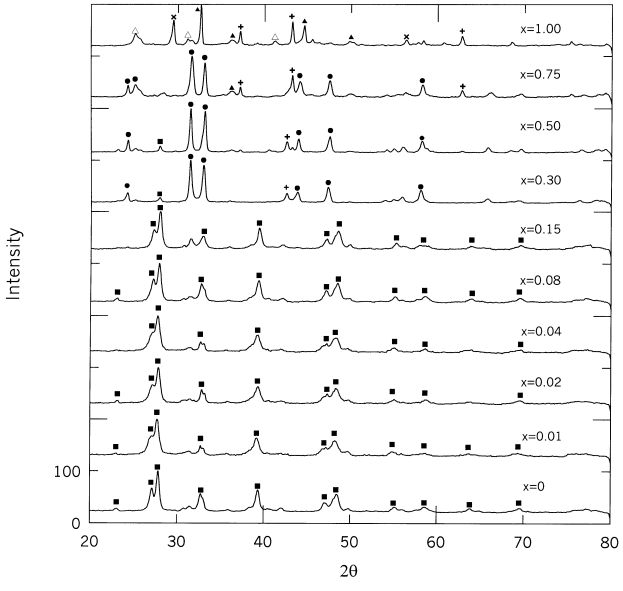

Fig. 5. XRD analyses for $La_{2(1-x)}NiSr_{2x}O_4$ with different x that calcined at 1073 K for 8 h. (■ La_2NiO_4, ● $La_{1.5}NiSr_{0.5}O_4$, + NiO, × SrO, ▲ $SrNiO_3$, △ Ni_2O_3.).

3.5. The properties of the sintered bodies

3.5.1. Measurement of resistivity

The changes in the resistivities increased for Sr^{2+} doped $LaNiO_3$ but decreased for La_2NiO_4.

The resistivity of $La_{2(1-x)}NiSr_{2x}O_4$ with various x values at room temperature is listed in Table 1. The resistivities for La_2NiO_4 were decreased really but were not proportional with the amount of Sr^{2+} dopant. It means from Fig. 7 that Sr^{2+} could enhance the ratio of Ni^{3+}/Ni^{2+} in La_2NiO_4. For the irregular characteristics that seem to derive from various factors, such as bulk densification and phase content, resistivity behaviour need further clarification. Data in Fig. 7 show that

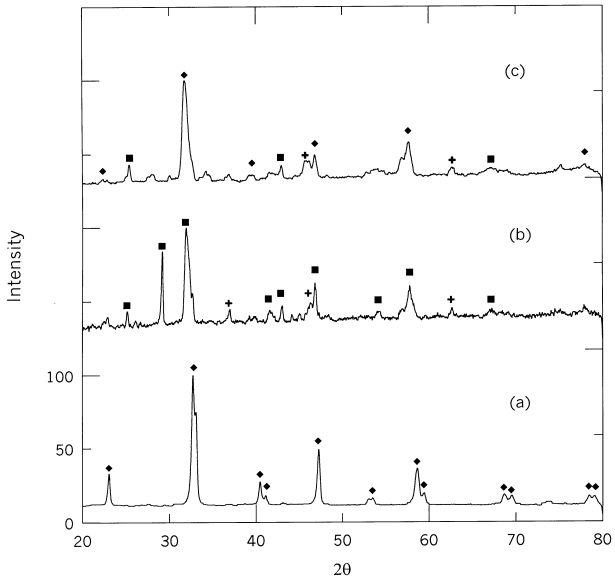

Fig. 6. XRD analyses for (a)$LaNiO_3$ calcined at 1073 K, (b)$LaNiO_3$ sintered at 1473 K and (c) $La_{1-x}NiSr_xO_3$ ($x=0.04$) sintered at 1473 K. (◆ $LaNiO_3$, ■ La_2NiO_4, + NiO.).

Table 1
Resistivities of $La_{2(1-x)}NiSr_{2x}O_4$ with different x

$La_{2(1-x)}NiSr_{2x}O_4$	
X	Resistivity Ω•m
0	2.80×10^{-3}
0.02	7.08×10^{-3}
0.04	4.47×10^{-3}
0.08	1.15×10^{-3}
0.15	1.26×10^{-3}
0.30	3.16×10^{-4}
0.50	3.30×10^{-4}
0.75	7.21×10^{-4}

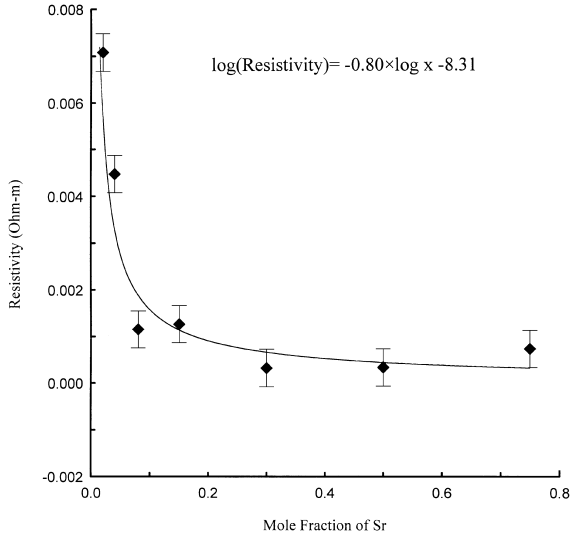

Fig. 7. Variation in the resistivity of the samples over mole fraction of Sr-doping.

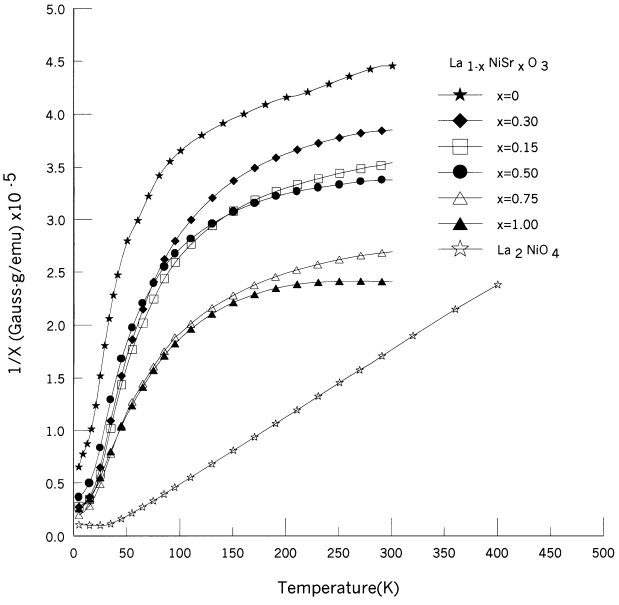

Fig. 8. SQUID analysis for $La_{1-x}NiSr_xO_3$ with different x value.

continuous $x=0.30$ and $x=0.50$ have lower resistivities than the others. It is to be considered that $La_{1.5}NiSr_{0.5}O_4$ is found from the XRD analysis as Sr^{2+} doping is between 0.30 and 0.50 in Fig. 5. Finally, the increasing of resistivity is that the NiO is dominant as Sr^{2+} doping is 0.75. We concluded that the resistivity is 2.80×10^{-3} Ω•m for La_2NiO_4 and 3.16×10^{-4} Ω•m for $La_{1.4}NiSr_{0.6}O_4$, respectively.

3.6. Magnetic determination

SQUID was used to measure the reciprocal of susceptibility with temperature [20] and the results are shown in Fig. 8. These appear to be Pauli paramagnetism

Table 2
Mass susceptibility of $La_{1-x}NiSr_xO_3$ with different **x**

$La_{1-x}NiSr_xO_3$	
x	Mass susceptibility (emu/Gauss-g)
0–0.08	$(2.11\pm0.05)\times10^{-6}$
0.15	2.83×10^{-6}
0.30	2.60×10^{-6}
0.50	3.01×10^{-6}
0.75	3.72×10^{-6}
1.00	4.17×10^{-6}

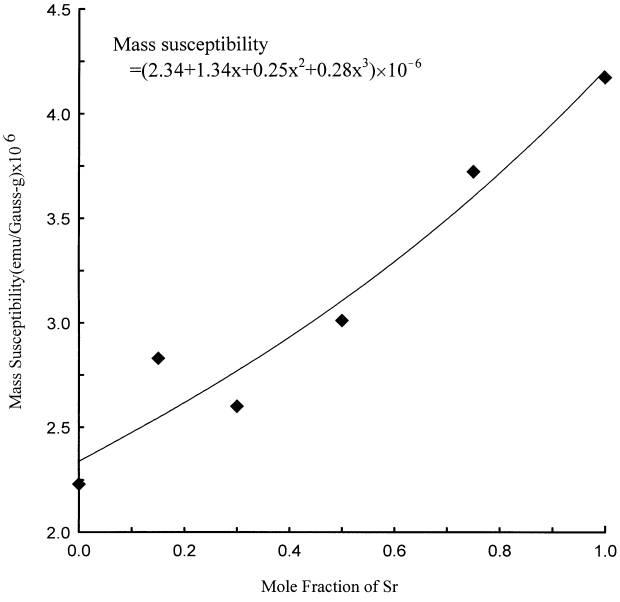

Fig. 9. Variation in the mass susceptibility of $La_{1-x}NiSr_xO_3$ with different mole fraction of Sr-doping.

for $La_{1-x}NiSr_xO_3$ ($x>0$) and antiferromagnetic behaviour for La_2NiO_4 from the shape of the curves. Doping Sr^{2+} to $LaNiO_3$ showed the same characteristics with $LaNiO_3$ and there were some deviations from normal $LaNiO_3$ at variant x value. For increasing in Sr^{2+}-doping the NiO and $La_{1.5}NiSr_{0.5}O_4$ phases emerged that would increase the susceptibility. The mass susceptibility of $La_{1-x}NiSr_xO_3$ with different x value was shown in Table 2. It was 2.11×10^{-6} (emu/Gauss-g) for $x=0$-0.08 and 4.17×10^{-6} (emu/Gauss-g) for $x=1.00$. The variation in the susceptibility of the samples over mole fraction of Sr is shown in Fig. 9.

4. Conclusion

1. The $La_{1-x}NiSr_xO_3$ and $La_{2(1-x)}NiSr_{2x}O_4$ can be obtained from coprecipiting with NaOH in about 0.2–0.4 M of corresponding metal chlorides in ethyl alcohol solution. The particle size of these oxides was at 0.1 μm. Alcohol as coprecipitating

solvent gives a better dispersion effect in this process and it can be recovered for recycle purposes.

2. According to the experimental results, the limit amount of doped Sr^{2+} for $La_{1-x}NiSr_xO_3$ and $La_{2(1-x)}NiSr_{2x}O_4$ was 0.15 and 0.30, respectively. Further doping Sr^{2+} would cause other compounds, such as $La_{1.5}NiSr_{0.5}O_4$, appearing in mixing type of oxides.
3. Owing to the effect of doped Sr^{2+} that could reduce the Ni^{3+} convert to Ni^{2+}. The $LaNiO_3$ that doped Sr^{2+} would maintain its perovskite phase at higher temperature.
4. The BET surface area of $LaNiO_3$ and La_2NiO_4 were 5.3156 (m^2/g) and 24.5857 (m^2/g), respectively. The results provide for the further research in the application of catalyst for other specific reaction.
5. The resistivities for La_2NiO_4 that doped Sr^{2+} were decreased but not for $LaNiO_3$. The resistivity was 2.80×10^{-3} Ω·m for La_2NiO_4 and 3.16×10^{-4} Ω·m for $La_{2(1-x)}NiSr_{2x}O_4$ ($x=0.30$).
6. Doping Sr^{2+} to $La_{1-x}NiSr_xO_3$ showed that it is the Pauli paramagnetism characteristics. The mass susceptibility of $La_{1-x}NiSr_xO_3$ with different x was 2.11×10^{-6} (emu/Gauss-g) for $x=0$–0.08 and 4.17×10^{-6} (emu/Gauss-g) for $x=1.00$.

Acknowledgement

The authors thank the National Science Council, NSC88-2214-E-006-016, for the financial support of this work.

References

[1] R.N. Singh, L. Bahadur, J.P. Pandey, S.P. Singh, P. Chartier, G. Poillerat, Preparation and characterization of thin films of $LaNiO_3$ for anode application in alkaline water electrolysis, J. App. Electrochem. 24 (1994) 149–156.
[2] H.S. Spacil, C.S. Tedmon, Electrochemical behavior of the perovskite-type $Nd_{1-x}Sr_xCoO_3$ in an aqueous alkaline solution, J. Electrochem. Soc. 122 (1975) 159.
[3] J. Drennan, C.P. Tavares, B.C.H. Steele, An electron microscope investigation of phase in the system La-Ni-O, Mater. Res. Bull. 17 (1982) 621–626.
[4] T. Kai, T. Takahashi, Kinetics of the methanation of carbon dioxide over a supported Ni-La_2O_3 catalyst, Canadian J. Chem. Eng. 66 (1988) 343–347.
[5] M.P. Rosynek, D.T. Magnuson, Prearation and characterization of catalytic lanthanum oxide, J. Catalysis 46 (1977) 402–413.
[6] K.R. Barnard, K. Foger, T.W. Turney, R.D. Williams, Lanthanum cobalt oxide oxidation catalysts derived from mixed hydroxide precursors, J. Catalysis 125 (1990) 265–275.
[7] H. Obayashi, Y. Sakurai, T. Gejo, Perovskite-type oxide as ethanol sensors, J. Solid State Chem. 17 (1976) 299.
[8] J. Tamaki, T. Maekawa, S. Matsushima, N. Miura, N. Yamazoe, Ethanol gas sensing properties of Pd-La_2O_3-In_2O_3 thick film element, Chem. Lett. 3 (1990) 477–480.
[9] P. Odier, Y. Nigara, J. Coutures, Phase relations in the La-Ni-O system: influence of temperature and stoichiometry on the structure of La_2NiO_4, J. Solid State Chem. 56 (1985) 32–40.
[10] C.N.R. Rao, D.J. Buttrey, N. Otsuka, P. Ganguly, H.R. Harrison, C.J. Harrison, J.M. Honig, Crystal structure and semicoductor-metal transition of the quasi-two-dimensional transition metal oxide, La_2NiO_4, J. Solid State Chem. 51 (1984) 266–269.
[11] R.D. Sanchez, J. Rivas, F. Garcia-Sanz, M.T. Causa, Approximation to the metal-insulator transition by Gd^{3+} doping in Pauli $LaNiO_3$ perovskite, J. Alloys and Compounds 239 (1996) 31–33.
[12] T. Nakamura, G. Petzow, L.J. Gauckler, Stability of the perovskite phase $LaBO_3$ (B= V, Cr, Mn, Fe, Co, Ni) in reducing atmosphere, 1. Experimental results, Mater. Res. Bull. 14 (1979) 649–659.
[13] K. Sreedhar, J.M. Honig, M. Darwin, M. Mcelfresh, P.M. Shand, J. Shand, B.C. Crooker, J. Spalek, Electronic properties of the metallic perovskite $LaNiO_3$: correlated behavior of 3d electrons, Phys. Rev. B 46 (10) (1992) 6382–6386.
[14] A. Li, C. Ge, P. Lu, N. Ming, Preparation of perovskite conductive $LaNiO_3$ films by metalorganic decomposition, Appl. Phys. Lett. 68 (10) (1996) 1347–1349.
[15] G. Demazeau, B. Buffat, M. Pouchard, P. Hagenmuller, Stabilization of unusual electronic configurations of transition elements in elongated six-coordinated oxygen sites of a K_2NiF_4 structure, J. Solid State Chem. 54 (1984) 389–399.
[16] P. Ganguly, C.N.R. Rao, Electron transport properties of transition metal oxide systems with the K_2NiF_4 structure, Mater. Res. Bull. 8 (1973) 405–412.
[17] C.-F. Kao, C.-L. Jeng, Preparation and characterization of lanthanum nickel oxide by combined coprecipitation and molten salt reactions, Ceram. Int. 25 (4) (1999) 375–382.
[18] V.F. Savchenko, L.S. Ivashkevich, I.Ya. Lyubkina, Preparation and electrical properties of solid solutions of the La_2O_3-NiO-BaO system, Inorg. Mater. 23 (6) (1987) 867–870.
[19] V.F. Savchenko, L.S. Ivashkevich, V.N. Meleshko, Solid solution in La_2O_3-Fe_2O_3-MO (M = Ni, Cu) systems, Inorg. Mater. 22 (7) (1986) 991–993.
[20] V.F. Savchenko, L.S. Ivashkevich, V.N. Meleshko, Phase transformations in the systems La_2O_3-Al_2O_3-MO (M = Ni,Cu), Inorg. Mater. 21 (10) (1985) 1499–1501.
[21] D.J. Buttrey, H.R. Harrison, J.M. Honig, R.R. Schartman, Crystal growth of Ln_2NiO_4 (Ln = La, Pr, Nd) by skull melting, J. Solid State Chem. 54 (1984) 407–413.
[22] H.R. Harrison, R. Aragon, C.J. Sandberg, Single crystal growth of the transition metal monooxide by skull melting, Mater. Res. Bull. 15 (5) (1980) 571–580.
[23] J. Takahashi, T. Toyoda, T. Ito, M. Takatsu, Preparation of $LaNiO_3$ powder from coprecipitated lanthanum-nickel oxalates, J. Mater. Sci. 25 (1990) 1557–1562.
[24] K. Vidyasagar, J. Gopalakrishan, C.N.R. Rao, Synthesis of complex metal oxides using hydroxide, cyanide and nitrate solid solution precursors, J. Solid State Chem. 58 (1985) 29–37.
[25] J. Takahashi, T. Toyoda, T. Ito, M. Takatsu, Preparation of $LaNiO_3$ powder from coprecipitated lanthanum-nickel oxalates, J. Mater. Sci. 25 (1990) 1557–1562.
[26] M.E. Baydi, S.K. Tiwari, R.N. Singh, J.L. Rehspringer, P. Chartier, J.F. Chartier, G. Poillerat, High specific surface area nickel mixed oxide powders $LaNiO_3$ (perovskite) and $NiCo_2O_4$ (spinel) via sol-gel type routes for oxygen electrocatalysis in alkaline media, J. Solid State Chem. 116 (1995) 157–169.
[27] Z.-Y. Zheng, B.-J. Guo, X.-M. Mei, A new technology of coprecipitation combined with high temperature melting for preparing single crystal ferrite powder, J. Magnetism and Magnetic Materials 78 (1989) 73–76.
[28] S.L. Dole, R.W. Scheidecker, L.E. Shiers, M.F. Berard, O. Hunter Jr, Technique for preparing highly-sinterable oxide powders, Mater. Sci. Eng. A 32 (1978) 277–281.

[29] S. Chikazumi, S.H. Charap, Physics of Magnetism, John Wiley and Sons, New York, 1964 (pp. 79–99, Chapter 5).
[30] L.M. Gan, H.S.O. Chan, L.H. Zhang, C.H. Chew, B.H. Loo, Preparation of fine $LaNiO_3$ powder from oxalate precursors via reactions in inverse microemulsion, Mater. Chem. Phys. 37 (1994) 263–268.
[31] W.W.M. Wendlandt, Thermal Analysis, third ed., John Wiley and Sons, New York 1985, pp. 147–184.
[32] J. Sun, T. Kyotani, A. Tomita, Preparation and characterization of lanthanum carbonate hydroxide, J. Solid State Chem. 65 (1986) 94–99.
[33] S. Bernal, F.J. Botana, R. Garcia, J.M. Rodriguez Izquiedo, Thermal evolution of a sample of La_2O_3 exposed to the atmosphere, Thermochim. Acta 66 (1983) 139–145.
[34] J. Drennan, C.P. Tavares, B.C.H. Steele, An electron microscope investigation of phases in the system La-Ni-O, Mater. Res. Bull. 17 (1982) 621–626.
[35] D.W. Johnson Jr., P.K. Gallagher, Reactive powders from solution in ceramic processing before firing, in: G.Y. Onada Jr., L.L. Hench (Eds.), Ceramic Processing Before Firing, John Wiley and Sons, New York, 1978, pp. 125–139.
[36] M.J. Sayagues, R.M. Vallet, A. Caneiro, A. Garcia, C.J.M. Gonzalez, Microstructural study of the $LaNiO_{3-x}$ system, Institute of Physics Conference Series 119 (1991) 315–318.